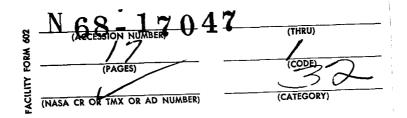
INFLUENCE OF INITIAL LOADING OF DIFFERING DEGREE AND DIFFERING FREQUENCY ON THE FATIGUE STRENGTH OF DRILLED FLAT BARS OF STEEL St 37.

PART B: MULTISTAGE AND SERVICE STRENGTH TESTS



Translation of "Finfluss unterschiedlich hoher und häufiger Vorbelastungen auf die Schwingfestigkeit gebohrter Flachstäbe aus St 37. Teil B: Mehrstufen- und Betriebsfestigkeitsversuche". Laboratorium für Betriebsfestigkeit, Darmstadt, Report No.FB-58, 1966. Pages 1-20 only

LABORATORY FOR SERVICE STRENGTH TESTING DARMSTADT

Report No.FB-58(1966)

E.Gassner and W.Schutz

INFLUENCE OF INITIAL LOADING OF DIFFERING DEGREE AND DIFFERING FREQUENCY ON THE FATIGUE STRENGTH OF DRILLED FLAT BARS OF STEEL St 37.

PART B: MULTISTAGE AND SERVICE STRENGTH TESTS

FRAUNHOFER SOCIETY
FOR ADVANCEMENT OF APPLIED RESEARCH

TABLE OF CONTENTS

- 1. Experimental Program
- 2. Summary of the Results
 - 2.1 Single-Stage Tests
 - 2.2 Initial Loading Tests, Service Strength Tests
- 3. Discussion of the Results
- 4. Details of the Results
 - 4.1 Stress Ratio n = -1
 - 4.2 Initial Loading Tests at n > -1
 - 4.3 Calibration Tests
 - 4.4 Raised Runaways
- 5. Cumulative Damage Hypotheses
- 6. Experimental Procedure

INFLUENCE OF INITIAL LOADING OF DIFFERING DEGREE AND DIFFERING FREQUENCY ON THE FATIGUE STRENGTH OF DRILLED FLAT BARS OF STEEL St 37. PART B: MULTISTAGE AND SERVICE STRENGTH TESTS

<u>/1**</u>

E.Gassner and W.Schutz

ABSTRACT. Experiments for determining the fatigue strength of drilled flat steel bars, under the influence of various initial stresses in multistage and operating strength tests. are discussed. The individual tests are described in detail. giving the load cycles, stress ratios, testing frequencies, and type of material (tempered and untempered bars). Cumulative damage hypotheses, specifically the Palmgren-Miner rule. are critically evaluated and disproved.

1. Experimental Program

The experimental program was established in close collaboration with Headquarters of the Federal Railroad in Munich and, insofar as intermediate results were desired, was modified or expanded. To obtain as complete as possible a view over initial loading, the following factors were successively varied:

Initial loading $V = \frac{n_1}{N_1} \cdot 100$

horizon $\sigma_{a,l}$

Initial stress horizon $\sigma_{\mathbf{a},\mathbf{l}}$ Ultimate stress horizon $\sigma_{\mathbf{a},\mathbf{l}}$ (always $< \sigma_{\mathbf{a},\mathbf{l}}$)

Stress ratio $\varkappa = \frac{\sigma_{\mathbf{u}}}{\sigma_{\mathbf{0}}}$ Testing frequency at the initial stress horizon $\sigma_{\mathbf{a},\mathbf{l}}$ See also Fig.1 and "Concepts and Definitions", which are given on a fold-out page at the end of this report*.

In addition, tests with cyclic initial loading were made.

1.1 Initial Loading $V = \frac{n_1}{N_1} \cdot 100$

The investigated range of initial loading $V = \frac{n_1}{N_1}$ covered 0.077% to 40%.

Originally, only tests with V = 5, 10, and 25% initial loading were planned since it was assumed that initial stresses lower than 5% have no influence on

^{*} Missing from original.

^{**} Numbers in the margin indicate pagination in the foreign text.

the yield strength and fatigue limit. This assumption was found erroneous; even at initial loadings of less than 1%, the yield strength and fatigue limit decrease at $\kappa = -1$.

1.2 Initial Stress Horizon σal

For the initial stress horizon σ_{al} , the steel St 37 used in the test has limitations because of its low ultimate tensile strength of about 26 kg/mm² and its relatively elevated fatigue limit in the notched state of about a value of ± 12 kg/mm²*. This entire region was covered by the initial stress horizons /2 σ_{al} = ± 24.0 , ± 17.0 , ± 14.0 , and ± 12.5 kg/mm² at μ = -1 and ± 14.0 as well as ± 12.5 kg/mm² at other stress ratios.

1.3 Ultimate Stress Horizon $\sigma_{a,2}$

The original program provided for an ultimate stress horizon of $\sigma_{\bullet,2}$, furnishing a lifetime of 2 × 10^6 load cycles. The practical difficulties in defining this horizon, even with a large number of tests, could not be overcome at first since excessive scattering occurred at these load cycles. Therefore, the ultimate stress horizon was so selected that the preloaded bars, at a life expectancy of 90%, reached a lifetime of 6 × 10^5 load cycles. We had planned to extrapolate the results to the desired 2 × 10^6 ultimate load cycles.

later, we used the so-called step method [(Ref.23, 22); description given elsewhere (Ref.1)]**which, in difference of the conventional methods, permits determining the yield strength or fatigue limit at a certain ultimate load cycle. The experimental program was then modified to accommodate this method.

If, for a certain value of V and $\sigma_{a,l}$, several ultimate stress horizons $\sigma_{a,2}$ are in question, "Wöhler curves for the prestressed test bar" can be plotted. This was possible at various occasions.

1.4 Stress Ratio $n = \frac{\sigma_u}{\sigma_0}$

Most of the test series were made at purely cyclic loading, i.e., at n = -1, while other series were carried out at n = -0.5, n = -0.2, n = -0.12, and n = 0. At the two latter stress ratios, the investigations could be made only in the fatigue limit region since otherwise the harmonic stress would have exceeded the ultimate tensile strength in the net cross section.

^{*} We intentionally omitted tests with $\sigma_0 > \sigma_s$ for principal reasons since, in practical use, one does not calculate with nominal stresses above the ultimate tensile strength.

^{**} References missing from original.

1.5 Testing Frequency of Initial Loading

For practical reasons, low initial loadings V cannot be applied at high frequency. Consequently, for load cycles of $n_1 < 4000$, we used a frequency of about 0.1 Hz. The extensive literature (Ref.2 - 21, 24 - 32), of which only /3 a small portion will be discussed in Section 6, did not indicate whether the frequency at which the initial loading is performed might have an influence on the damage done to the test bar. However, during the tests it was found that a low frequency (≈ 0.1 - 0.2 Hz) damages the initial loading more than a high frequency (≈ 30 Hz), despite the fact that practically no differences in lifetime were produced by the differing test frequencies in the single-stage tests.

As had been reported in Part A (Ref.1), the tests were made with the MR St 37-2 steel and with axially loaded drilled flat bars. The plates from which the specimens were taken came from the same charge as those described in Part A.

In planning the tests, it had to be considered that, generally, the scattering of the ultimate load cycles is greater in initial loading tests than in single-stage tests. If this fact is not allowed for by a sufficiently large number of initial loading tests, thus making a statistical evaluation possible, wrong conclusions might be obtained.

Specifically, the Wöhler curve as reference line must be determined with great accuracy. This can be attained by stipulating a uniformly high quality of the bore surfaces, reproducible over a period of several years. Originally, this requirement had not been met in the bores produced by the Federal Railroad Repair Works Freimann; for this reason, the test bars were subsequently purchased from Gebr. Frisch K.G. who improved the bore surface considerably. It is true that the corresponding Wöhler curves no longer coincided accurately at ultimate load cycles $> \approx 10^6$. For this reason, the initial loading tests with the so-called "Federal Railroad" bars must be referred to the Wöhler curves of the "Federal Railroad" bars while the tests made with the so-called "Frisch" bars must be referred to the Wöhler curves of the "Frisch" bars

In addition, high constancy of the testing forces is necessary.

2. Summary of the Results

More details will be given in Sections 3 and 4 or can be taken from the graphs in the Appendix. The results of the Wöhler tests (Ref.1) are repeated here insofar as they have a bearing on the initial loading tests. It is suggested, in reading the following Sections, to make use of the fold-out page "Concepts and Definitions" at the end of this paper.

2.1 Single-Stage Tests

2.1.1 The Wöhler curve for n = -1 is a straight line $N = C \cdot \overline{\sigma}_a^k$ in the

^{*} Missing from original.

range from 10^4 to 4×10^5 ultimate load cycles. The exponent k, determining the slope of the Wöhler curve, is about 6.8.

- 2.1.2 The mean scattering range $T_N^* = \frac{N_{90}}{N_{10}}$ has an approximately constant value of $T_N^* = 1:1.7$ between 10^4 and 4×10^5 load cycles; this corresponds to a scattering range of the stress amplitudes $T_0^* = \frac{\sigma_{a,90}}{\sigma_{a,10}}$ of about 1:1.1. Within the fatigue-limit region, the mean scattering range T_0^* also is about 1:1.1.
- 2.1.3 The 50% values of the tolerable stress amplitudes at 1×10^6 and 2×10^6 load cycles differ only negligibly for the "Frisch" bars. In other words, the Wöhler curve is almost horizontal, starting from N = 1×10^6 . In the "Federal Railroad" bars, the horizontal branch of the Wöhler curve is not yet reached at 2×10^6 load cycles.
 - 2.1.4 The mean stress sensitivity M is extremely low, being 0.54 0.55.
- 2.1.5 The stress amplitudes, tolerable from the viewpoint of yield strength and fatigue limit, especially in the notched state, are high compared with the literature data (Ref.16, 33, 34). This is true for all stress ratios κ from -1 to 0.
- 2.1.6 The testing frequency has practically no influence on the ultimate load cycles in single-stage tests.
- 2.1.7 If the test bars are annealed so as to reduce the internal strains set up by the drilling process, both yield strength and fatigue limit will $\frac{1}{2}$ decrease. Since the small internal strains produced by the drilling have no influence on the lifetime at ultimate load cycles of N < $\frac{1}{4}$ × 10⁵, it is obvious that the annealing must have produced other harmful effects. [The tests made with annealed bars had not been described in our first paper (Ref.1).]
- 2.1.8 The testing forces were kept extremely constant over a period of four years. Calibration series run at intervals of 4-5 months, with 8-10 individual tests each, showed no significant differences in the ultimate load cycles.

2.2 Initial Loading Tests. Service Strength Tests

- 2.2.1 The decrease in yield strength and fatigue limit or endurance limit, produced by a certain initial loading V, i.e., the damage S_{σ} resp. S_{N} , is generally independent of the initial stress horizon $\sigma_{a,l}$. Only on approach of $\sigma_{a,l}$ to the fatigue limit will the damage decrease.
- 2.2.2 Already an initial loading of < 1% will lower both yield strength and fatigue limit.
- 2.2.3 The "Wöhler curve of the prestressed bar", in single-stage initial loadings. runs approximately parallel to the normal Wöhler curve in the entire

yield-strength and fatigue-limit region; in multistage initial loadings, this curve is considerably steeper.

- 2.2.4 If the initial loading is done in three stages $\sigma_{a,11} > \sigma_{a,12} > \sigma_{a,13}$, the damage S_{σ} will depend on the ultimate stress horizon $\sigma_{a,2}$; in this case, S_{σ} cannot be found by simple addition of the damages of the individual stages; it is especially in the region of higher ultimate load cycles n_2 that we obtain a value of $S_{\sigma,tot} > S_{\sigma,1} + S_{\sigma,2} + S_{\sigma,3}$.
- 2.2.5 If the multistage initial loading, mentioned in paragraph 2.2.4, is applied as a mixed load in eight subcycles, no changes in the result are produced.
- 2.2.6 Four-stage service strength tests in which, in contrast to the above-mentioned tests, the total stress frequency distribution is passed repeatedly in an ascending and descending manner until failure takes place, produced no different endurance limits than in the tests according to paragraphs 2.2.4 and 2.2.5.
- 2.2.7 If a fifth stage is added to the four-stage service strength test described in paragraph 2.2.6, with this additional stage located at about 45% of the fatigue limit, no changes of the result for the investigated load cycle region are observed.
- 2.2.8 At the stress ratios used, an initial loading at n=0 produces the least damage. This can be explained by the build-up of favorable internal strains.
- 2.2.9 The "cumulative damage hypothesis" by Palmgren-Miner (Ref.35, 36) furnished relatively uncertain results in almost all test series. The obtained damage sums $\sum \frac{n_i}{N_i}$ are especially low whenever the ultimate stress horizon $\sigma_{a,e}$ was below the fatigue limit (for example, in initial loading tests $\sum \frac{n_i}{N_i} = 7.7 \times 10^{-4}$; in service strength tests $\sum \frac{n_i}{N_i} = 7.7 \times 10^{-2}$). However, these sums are unable to attain a value of $\sum \frac{n_i}{N_i} = 1.0$ even when all applied stress amplitudes are higher than the fatigue limit; in this case, the lowest value is $\sum \frac{n_i}{N_i} = 0.35$. Even if the stress amplitudes, located below the fatigue limit, are taken into consideration, the damage sum will frequently remain below 1.0.
- 2.2.10 Initial loading at low frequency (0.1 0.2 Hz, "slow start") will produce more damage than loading at high frequency (30 Hz, "rapid start").
- 2.2.11 Equal initial loading V will produce approximately the same damage in annealed as in unannealed bars.
 - 2.2.12 The tolerable stress amplitudes in the fatigue-limit region and the

ultimate load cycles in the yield-strength region scatter more in the initial loading tests than in the single-stage tests.

3. Discussion of the Results

The experimental program with all necessary details is given in Tables 1 to 4. The damage S_{σ} , i.e., the decrease in tolerable stress amplitudes due $\frac{7}{2}$ to the initial loading V, is shown in Fig.3 where the results of all test series are compiled. To obtain as large as possible a number of test points, we made the following assumption, originally formulated by Webber and Levy (Ref.5) and later checked in practical measurements by Gassmann (Ref.37):

A test bar, whose ultimate load cycle or tolerable stress amplitude during initial loading tests is located near the lower respectively the upper scattering limit, will break already in a single-stage test at the lower respectively upper scattering limit.

Under this assumption, it is possible to accurately define the initial loading of each individual bar which, because of the scattering of the ultimate load cycles in the Wöhler experiment, must always be correlated with a certain survival probability. A typical example is shown in Fig.4: Ten test bars were subjected to initial loading at $\sigma_{a,l}$ with $n_1 = 10^4$ load cycles. In that case, the initial loading, depending on the survival probability for which it is to be valid, will be $V_{50} = 10.0\%$; $V_{90} = 12.5\%$; and $V_{10} = 8.0\%$. The ultimate load cycles of the ten bars at $\sigma_{a,2}$ are as follows: $n_{2,50} = 10^6$, $n_{2,90} = 7 \times 10^5$, and $n_{2,10} = 10^6$.

These load cycles are tolerated by equivalent test bars in the Wöhler test at stress amplitudes of $\sigma_{a,3,50}$; $\sigma_{a,3,90}$; and $\sigma_{a,3,10}$. A test bar which, for example, breaks at a load cycle of $n_2 = 7 \times 10^5$ according to $P_s = 90\%$, would have reached 8×10^4 load cycles at $\sigma_{a,1}$ in the Wöhler test; consequently, this bar had undergone an initial stress of

$$V_{90} = \frac{10^4}{8 \cdot 10^4} = 12.5 \%$$

leading to a damage of

$$s_{\alpha,90} = \frac{\sigma_{\alpha,3,90} - \sigma_{\alpha,2}}{\sigma_{\alpha,3,90}}$$
.

The described procedure is especially suitable for the step method since, in this case, the tolerable stress amplitudes of the Wöhler series and the initial stress series, at equal critical load cycle (usually 2×10^6) are directly comparable.

The damage S_N can be calculated in a similar manner. However, this can be defined only if the ultimate stress horizon $\sigma_{a,2}$ is above the fatigue limit; in other cases, we have $S_N=0$.

Both methods (determination of S_{σ} or S_{N}) furnish useful results only if

the scattering in the initial loading test is greater than in the single-stage test since otherwise the completely illogical result would be obtained that a greater initial loading would cause a smaller damage. Tables 5 and 6 show that

the scattering values $T_N = \frac{N_{90}}{N_{10}}$ and the standard deviations s of the initial

loading tests generally meet the above requirement, aside from a few exceptions. The mean numerical values are $T_N^{\star}=1:2.4$ and $s_0^{\star}=0.532~\mathrm{kg/mm^2}$ in initial loading tests, compared with $T_N^{\star}=1:1.7$ and $s_0^{\star}=0.36$ in single-stage tests.

Figure 3 refers to the damage S_σ ; from each experimental series, three individual points V_{90} , V_{50} , and V_{10} were calculated and plotted at the corresponding damage $S_{\sigma,90}$, $S_{\sigma,50}$, and $S_{\sigma,10}$.

Most of the test points for κ = -1 are located within a relatively narrow scattering range which shows a damage already at initial loadings of \approx 0.1%. The initial stress horizon σ_{a1} = ± 12.5 kg/mm² produces less damage, presumably because of the fact that it is very close to the fatigue limit of ± 12.4 kg/mm² (P_{s} = 50%).

Test bars, prestressed at n > -1, show less damage; in part, the tolerable stress amplitudes even increase, presumably because of the favorable (compressive) internal strains which are set up especially at n = 0 by the first load cycles during the initial loading and which are not at all, or only slowly, broken down by the subsequent load cycles (Ref.38, 39). In addition, it can be suspected that, at the periphery of the bore, the material is plasticized and thus cold-worked by the high harmonic stresses occurring at n = 1, a fact which partly masks the effect of damage.

The relatively great scattering (see Table 5) observed in these experiments could possibly be attributed to internal strains whose extent and magnitude would depend on the local ultimate tensile strength of each individual bar at the point of maximum stress. Since microscopic regions are involved here, the ultimate tensile strength might scatter strongly.

Similarly, bars subjected to a stress-relief anneal are located within the scattering zone.

Bars subjected to multistage initial loading generally show much greater damage than would have been expected from a simple addition of the initial stresses. Details are given in paragraphs 4.1.5 and 4.1.6.

If the above assumption is abandoned, the results can be represented as $\frac{9}{2}$ shown in Figs.5 - 7. All values refer to a survival probability of $P_s = 50\%$; the 50% value was selected since it is most accurately defined. This is true at least in cases in which a logarithmic normal distribution of the ultimate load cycles can be assumed, i.e., in the yield-strength region as long as no runaways occur. If these occur close to the fatigue limit, the ultimate load cycle will be more reliably known for a survival probability of $P_s = 90\%$. In the step method, the 50% value is most favorable. The latter method is especially suitable for determining the 50% value but less suitable for calculating the scattering and thus the 90% or 10% value (Ref.40).

damage than at a low testing frequency (\approx 0.1 to 0.2 Hz). As is logical, the results in Fig.7 scatter more since they refer to ultimate load cycles. Figure 7 contains only the test series whose ultimate stress horizon $\sigma_{a,2}$ is above the yield strength. In addition, curves of equal damage, according to Palmgren-Miner (Ref.35, 36), are plotted in Fig.7 which contains not only the curve for $\sum \frac{n_1}{N_1} = 1.0$ but also curves for other damage sums < 1.0; accordingly, individual test results attain only $\sum \frac{n_1}{N_1} \approx 0.4$ despite the fact that all stress

amplitudes are above the fatigue limit [this reservation had been made by Miner

The damage S_{σ} at 6 \times 10⁵ and 2 \times 10⁶ load cycles is shown in Figs.5 and 6

while the decrease in ultimate load cycle (damage S_N) is given in Fig.7. The results in Figs.5 and 6 deviate only slightly from a continuous curve, in which case initial loading at high testing frequency (\approx 30 Hz) generally produces less

It is logical to ask whether the differing damage produced by the testing frequency is statistically significant or not. The standard method (Ref.1) shows no significant differences between each two comparable series (see Table 7); however, the method does not consider that a large number of additional series, although at different initial loadings V, are in existence which also show a greater damage at low testing frequency. In other words, only a fraction of the information pointing toward a real rather than an accidental difference is actually used in the significance check. However, no statistical method is presently available that would permit use of these additional data /10 (Ref.41). Therefore, despite the negative result of the significance check, it is assumed that low testing frequencies produce greater damage than high frequencies. Since the Wöhler curve is practically uninfluenced by the testing frequency, it appears that the damage in the slow-start procedure first progresses more rapidly but later more slowly than in the rapid-start version.

4. Details of the Results

in his original paper of 1945 (Ref.36)].

The results of all initial loading tests are shown in Figs.8 - 23; tables containing all tests with the necessary details can be requested from the laboratory for Service Strength Testing(Laboratorium für Betriebsfestigkeit). In addition, Figs.8 - 23 give the corresponding Wöhler curves (for "Frisch" bars or "Federal Railroad" bars). All curves refer to a survival probability $P_{\rm s}$ = 50%; the corresponding ultimate load cycles are taken from the frequency evaluations of Figs.24 - 40, while the stress amplitudes for the step method are taken from Figs.41 - 58. More details on the statistical evaluation were given previously (Ref.1).

^{*} The same is true also for the comparison between Wöhler curve and prestressed bars in Table 7.

4.1 Stress Ratio n = -1

4.1.1 Initial Loading at $\sigma_{a,1} = \pm 24.0 \text{ kg/mm}^2$

This is the highest possible initial stress horizon, located already close to the ultimate tensile strength.

The results are plotted in Fig.8, and the frequency evaluations are shown in Fig.24.

The "Wöhler curve for the prestressed bar" runs approximately parallel to the normal Wöhler curve. The three series on this initial stress horizon must be considered only as subsidiary series since the fatigue limit most likely cannot be exceeded that far in practical work. All test bars were prestressed at low testing frequencies since the endurance limit in the single-stage test is only about 10⁴ load cycles and since the initial loads of 7.8 resp. 23.4% cannot be applied at high frequencies.

4.1.2 Initial Loading at $\sigma_{al} = \pm 17.0 \text{ kg/mm}^2$

/11

In this case, 12 series were carried out with initial loadings of 0.1 to 26% at low testing frequencies and of 4-40% at high frequencies. In the experimental program, this horizon was initially considered as the most important one, whereas later main emphasis was placed on the horizon $\sigma_{a,1}=14.0~{\rm kg/mm^2}$ discussed in Section 4.1.3. Two test series were carried out with the step method. Most of the test bars still had the "Federal Railroad" bore (see Table 1).

The results are plotted in Figs.9 and 10, while the frequency evaluations are given in Figs.25 and 26 and the step methods in Figs.41 and 42.

Primarily, the tests indicate that the testing frequency of the initial loading has an influence on the damage (see Fig.10). For example, the damage produced by V = 2.6% at ≈ 0.1 Hz is the same as that produced by V = 40% at ≈ 30 Hz. In addition, it was found that an initial loading of only 1% will decrease both yield strength and fatigue limit (see Figs.9 and 10). Since only one test series per initial loading is available, no "Wöhler curve for predamaged test bars" could be plotted. On the basis of the tests described in Section 4.1.3, it can be assumed, however, that these curves will be approximately parallel to the normal Wöhler curve.

As mentioned before, the tests had to be run in part with "Federal Railroad" bars and in part with "Frisch" bars. For the work discussed here it is of importance that both bars suffered approximately equal damage at equally large initial loading (see the two series with 10.4% initial loading at low testing frequency, given in Figs.9 and 10).

4.1.3 Initial Loading at $\sigma_{al} = \pm 14.0 \text{ kg/mm}^2$

The results of the 12 test series are plotted in Fig.11, while the fre-

quency evaluations are shown in Figs.27 and 28 and the step methods in Figs.43 to 45.

The tests covered 0.077 - 8.1% initial loading at 0.1 Hz and 7.7 - 19.2% initial loading at rapid start. In these test series, we usually selected several ultimate stress horizons so that the frequently mentioned "Wöhler curves for prestressed bars" can be given (see Fig.11).

These curves are approximately parallel to the original Wöhler curve. /12 Individual deviations such as, for example, of the curves for 0.077 and 0.77% initial loading at 0.1 Hz, presumably are due to scatterings of the test results. Here again, an initial loading at low testing frequency produces greater damage than at high testing frequency; for example, V = 0.77%, at slow start, will decrease the tolerable stress amplitudes just as much as V = 7.7% at rapid start.

Two test series with 8.1% initial loading each were made with "Federal Railroad" bars; these can be plotted also in Fig.11 (just as the other series) since, within the yield-strength region, the Wöhler curve for the "Federal Railroad" bars does not differ from the Wöhler curve for the "Frisch" bars.

Furthermore, it will be found that the height of the initial stress horizon has practically no influence on the damage (see, for example, the test series with V = 7.8% at ± 24.0 kg/mm²; V = 10.4% at ± 17.0 kg/mm²; V = 8.1% at ± 14.0 kg/mm² which all were made at a low testing frequency). In other words, an initial loading of, for example, 10.0% will produce equal damage, irrespective of the initial stress horizon.

4.1.4 Initial Loading at ±12.5 kg/mm²

The results of the three test series are plotted in Fig.12, while the frequency evaluation is shown in Fig.29 and the step method in Fig.47.

This initial stress horizon is located only slightly above the fatigue limit of $\pm 12.4~\rm kg/mm^2$ (2 × 10^6 load cycles, survival probability $P_s = 50\%$, "Frisch" bars). Since individual test bars, in the single-stage test, no longer break at $\pm 12.5~\rm kg/mm^2$, i.e., are not damaged even by an arbitrarily large load cycle, one had to expect from the very beginning a much greater scattering and several runaways. The frequency evaluations in Fig.29 confirm this assumption; here, three of nine resp. ten test bars show runaways at a stress amplitude of $\sigma_{a\beta} = \pm 11.8~\rm kg/mm^2$.

Similarly, it had to be expected that a certain initial stress does not produce the same extensive damage as at higher initial stress horizons. Since, in addition, the ultimate load cycles scatter especially much and thus render the results uncertain, it must be assumed that initial stresses close to the yield strength produce no damage.

4.1.5 Three-Stage Initial Loading at ±24.0. ±17.0. and ±14.0 kg/mm²

The results of the three test series are plotted in Fig.13, and the fre-

quency evaluations are given in Fig.30.

These experiments were to show the manner in which a multistage initial loading might produce damage. For this, the test bars were prestressed with a low frequency at ± 24.0 , ± 17.0 , and ± 14.0 kg/mm² with 7.7, 10.4, resp. 8.1%. An addition of the initial loadings yields a total of V=26.2%. Since three ultimate stress horizons are present, it became possible to plot a "Wöhler curve for prestressed bars"; this curve is no longer parallel to the original Wöhler curve but is much steeper (see Fig.13). Consequently, the damage depends here on the ultimate stress horizon (in contrast to the single-stage initial loading). For example, in the region of 2×10^5 ultimate load cycles, the tolerable stress amplitudes decrease by approximately the same amount as that observed in a single-stage initial loading of 26.0%. Conversely, at high ultimate load cycles ($\approx 2 \times 10^6$), they drop as much as in the single-stage initial loading of about 50%. This unexpected behavior has not yet been explained.

4.1.6 Three-Stage Initial Loading at ±17.0, ±14.0, and ±12.5 kg/mm²

The results of the three test series are plotted in Fig.14, while the frequency evaluations are given in Fig.31 and the step method in Fig.48.

The purpose of these test series was to stress the bars in a manner closer to actual service conditions than had been used in previous tests. Under service conditions, the fatigue limit is rarely exceeded by large amounts but often by small amounts. Therefore, the test bars of these series were subjected to initial loadings with about 1% at ± 17.0 kg/mm² (= 8.6×10^2 load cycles), 7.0% at ± 14.0 kg/mm² (= 3.0×10^4 load cycles), and 12.5% at ± 12.5 kg/mm² (= 1.5×10^5 load cycles). In this case, it was to be assumed that the initial loading at ± 17.0 kg/mm² would lower the fatigue limit so far (approximately to ± 11.5 kg/mm²) that even an initial loading at 12.5 kg/mm² produced considerable damage (in contrast to regular initial loading tests; see Sect.4.1.4).

As in the tests discussed in the preceding Section, the fatigue limit / \underline{U}_4 drops steeply, out of all proportion. On an addition of the damage done by V = 1.0% + 7.7% + 12.5% = 21.2%, a decrease in fatigue limit to about $\pm 11.0 \text{ kg/mm}^2$ must be expected according to Fig.6; in reality, however, not more than about $\pm 10.0 \text{ kg/mm}^2$ can be tolerated. If the initial loading, in contrast to the prior method, is subdivided into eight cycles (see Fig.2), no change in average endurance limit will take place.

The excessive scatter of the tests discussed in this Section (see Tables 5 and 6) can be explained as follows:

The single-stage tests show extensive scatter at σ_a = ±12.5 kg/mm² (Ref.1). This causes a highly inaccurate definition of the initial loading V at equal stress amplitude (see Table 2); the initial loading, in turn, fluctuates between V_{90} = 27.2% and V_{10} = 6.25%. Consequently, the results discussed in this Section exhibit some uncertainties.

4.1.7 Four- and Five-Stage Service Strength Tests

The results of the three test series are plotted in Fig.15, while the frequency evaluations are shown in Fig.32.

In Fig.15, the maximum value of frequency distribution $\overline{\sigma}_a$ is plotted against the total load cycle \overline{N} , as is conventional in service strength tests. In the row 13c, the load cycle referring to the fifth stage was disregarded.

The service strength test closely approaches actual service stresses of varying stress amplitudes. The frequency distribution is subdivided into several – usually eight – stages which, beginning with a central stage, are passed in an ascending and descending direction until rupture occurs (see Fig.2). In our studies, a four-stage (in one series, a five-stage) composite with a load cycle of $\bar{N}_1\approx 272,000$ resp. 525,000 per subcycle was selected (see Fig.16). It was originally assumed that the endurance limit of the test bars, at this frequency distribution, would be much greater than in the three-stage initial loading described in Section 4.1.6, partly because of the fact that the high stages producing the greatest damage are traversed in one pass and in descending sequence during the initial loading tests. As shown in Fig.17, this assumption /15 proved untrue. The tolerated frequency distributions are quite similar in both types of test.

A second test series was carried out at stress amplitudes which, in all stages, were 10% lower; this series had the purpose of deriving the so-called "endurance curve" for the test bar made of steel St 37. In normal eight-stage service strength tests, many of the materials showed an exponent $\bar{k}\approx 6.5$ for the endurance curve, which is independent of test parameters such as material, form factor, average stress, stress ratio, and type of stress, as could be proved by a large number of service strength tests (Ref.42). If the exponent \bar{k} is known, the results can be extrapolated from a high stress level, and thus a short life, to a low stress level and thus a longer life.

Conversely, the endurance curve for the existing four-stage frequency distribution has a much more shallow slope, showing an exponent of $\overline{k} \approx 14.0$. It can be assumed that this is more a consequence of the four-stage frequency distribution used here than of the material St 37.

Finally, we carried out a test series, containing a fifth stage at a value of 50% of the fourth stage, i.e., about 45% of the fatigue limit. Figures 15 and 17 show that this fifth stage, expressed in subcycles to rupture, has no influence on the endurance limit, meaning that the added fifth stage produces no damage at $\sigma_a = \pm 5.7 \text{ kg/mm}^2$.

4.1.8 <u>Single-Stage Tests and Initial Loading Tests with</u> Annealed Bars

The results of the three test series are plotted in Fig.18, while the step method is shown in Figs.49 and 50. The single-stage tests with annealed bars had not been reported in our earlier paper (Ref.1).

The single-stage tests resulted in a higher fatigue limit for the "Frisch" bars than for the "Federal Railroad" bars. This is due not only to the smoother bore surface but also to minor internal strains, set up by the friction. A few additional test series were to show the behavior of annealed bars in single-stage tests and in initial loading tests. The annealed bars, over the entire /16 region from 7×10^4 to 2×10^6 ultimate load cycles, showed lower tolerable stress amplitudes than had been expected at first (see Fig.18). Compared to the "Frisch" bars, the yield strength decreased by about 6.0% and the fatigue limit by about 13.0%. The tempering, which was done in a neutral salt bath at 680° C for 60 min, thus not only decomposed the internal strains but also had a detrimental effect on the fatigue strength behavior in the entire load cycle range. Ultimate tensile strength, tensile strength, and hardness of the material were not changed by the annealing.

Initial loading tests with tempered bars indicate (see Fig.18) that the damage S_{σ} is practically as great as in normal bars.

4.2 <u>Initial Loading Tests at n > -1</u>

4.2.1 Stress Ratio n = -0.5, -0.2, and -0.12

The results of the six test series are plotted in Figs.19 - 22, while the frequency evaluations are given in Fig.33 and the step method in Figs.51 - 55.

No Wöhler curves are available for $\kappa=-0.5$ and -0.12, but they can be estimated with fair accuracy from a fatigue-limit versus yield-strength diagram given in our earlier paper (Ref.l). The "Wöhler curve of bars damaged at $\kappa=-0.5$ " runs about parallel to the normal Wöhler curve; however, the damage itself is much less than for $\kappa=-1$. The same is true for tests at $\kappa=-0.12$ (see Fig.22). Conversely, test bars stressed at $\kappa=-0.2$ to two initial stress horizons $\sigma_{\rm al}$ showed considerable damage (see Figs.20 and 21).

4.2.2 Stress Ratio n = 0

The results of the three test series are plotted in Fig.23, while the step method is given in Figs.56 - 58.

At this stress ratio, internal strains are preferentially set up; since n = 0 (tension) is involved, these are favorable (compressive) internal strains. As expected, the initial loading produces practically no damage.

4.3 <u>Calibration Tests</u>

/17

The frequency evaluation is shown in Fig.34.

To monitor the constancy of testing forces over the entire experimental period of four years, we ran so-called calibration series at intervals of about four months at $\sigma_a = \pm 17.0 \text{ kg/mm}^2$, $\kappa = -1$. Eight of the series were discussed in our earlier paper (Ref.1); up to the end of the initial loading tests, one more

calibration series was run; see Fig. 34, in which also the frequency evaluation of all nine calibration series with a total of 99 tests is entered. The points are readily fitted by a straight line; for this reason, a logarithmic normal distribution of the ultimate load cycles can be assumed. No statistically significant deviation of the last series from all other calibration series was detected.

4.4 Raised Runaways

The frequency evaluations are shown in Figs.35 - 40.

Due to the many step methods used, numerous unruptured bars, known as "runaways" were present. These totaled 249 bars, all of which were tested to failure at the "calibration horizon" $\sigma_{\rm a}=\pm17.0~{\rm kg/mm^2}$, $\kappa=-1$, irrespective of whether they had been stressed in the single-stage or in the initial loading test, at $\kappa=-1$, or at any other stress ratios. All these runaways are interpreted in Fig.35, while the runaways of the individual initial loading series are shown in Figs.36 - 40. Up to a survival probability of $P_{\rm s}\approx83\%$, the runaways practically osculate a straight line which coincides with the normal Wöhler tests (no statistically significant difference). However, the curve deflects toward the left above the mentioned survival probability. This means that a certain percentage of the bars had been damaged by prior loadings. Practically no so-called trained bars, i.e., bars with an improved fatigue strength, were encountered. One single bar attained an unexpectedly high ultimate load cycle. A metallographic check test (see Fig.59) indicated that the surface of the bore showed extensive plastic strain.

5. Cumulative Damage Hypotheses

/18

In aircraft construction, the so-called "Palmgren-Miner rule" is frequently used $\left(\sum \frac{n_1}{N_1}\right) = 1.0$; see "Definitions and Symbols" for drawing conclusions from

Wöhler tests as to the endurance limit under statistically variant stresses. This hypothesis was originally formulated in 1924 by Palmgren (Ref.35) and applied in 1945 by Miner (Ref.36) for dimensioning aircraft structural parts. Miner himself restricted the validity of his rule by numerous reservations; later, the entire rule was frequently disregarded.

It was soon found (Ref.19, 29, 43) that the Palmgren-Miner rule is useless in most cases; cumulative damage between \ll 1 to ∞ may actually occur.

The main drawbacks of the Palmgren-Miner rule are as follows:

- 1) The damage process is assumed to have a linear course.
- 2) The variations in internal strain during the tests, as they might be produced by the sequence of stress amplitudes, are disregarded.
- 3) Stress amplitudes below the yield strength are not entered in the calculation.

In practical application, the following difficulty occurs:

In frequency distributions, as they occur in actual service, the "stress amplitudes of maximum damage" are located almost always close to the fatigue limit. However, it is only in a few cases that the fatigue limit itself is sufficiently well known for allowing a reliable calculation with the Palmgren-Miner method.

Today, it is no longer a question to decide whether the Palmgren-Miner rule is applicable or not, since it has been disproved in too many papers. The occasional occurrence of a cumulative damage ≈ 1.0 must be attributed to pure chance; even a minor change in a single parameter, such as the mean stress, may lead to entirely different damage sums (Ref.42).

The above-mentioned drawbacks were responsible for the fact that many investigators formulated their own cumulative damage hypotheses (Ref.2, 44-52) in which, at the expense of simplicity, attempts were made to obtain a better match between calculation and test results. We should mention here the method by Gatts (Ref.45) which allows for the influence of the sequence as well as for the stress amplitudes located below the fatigue limit.

Presumably, none of the more recent hypotheses will furnish correct /19 results; in addition, extensive and cumbersome tests are needed in many of such cases so that conventional service strength tests, which are quite independent of cumulative damage hypotheses, will become much more economical.

A recent paper makes the following statement as to the modern hypotheses (Ref.53):

"Some authors have stated that their particular methods are superior to the linear cumulative damage hypothesis; however, such 'superiority' is generally obtained by matching empirical constants to the existing — not generalizable — test results. Very few of the suggested relations make an attempt to allow for the true damage mechanism".

The same author also doubted that it would be possible in the near future to formulate a reliable cumulative damage hypothesis.

Despite this situation, we calculated the results of all our test series on the basis of Miner's rule (see Tables 1 - 4 and 8). As mentioned, depending on the selected test conditions, extremely low damage sums occur for the investigated material. It is logical that the Miner rule furnishes results of extreme

uncertainty, i.e., $\sum \frac{n_i}{N_i} < 1.0$, whenever the test bars above the fatigue limit

are exposed to relatively low, initial loads and subsequently are tested to rupture below the fatigue limit. However, even in the test series in which both stress amplitudes were located above the fatigue limit, a stipulation made by

Miner in his original paper, we almost always obtained a value of $\sum \frac{n_1}{N_1} < 1$.

Several eight-stage service strength tests with the LBF standard distribution, made after completion of our present study on request by the Federal Rail-

road Central Office (Ref.54), resulted in values of $\sum \frac{n_i}{N_i}$ = 0.27 for purely

cyclic stresses. This value is the lowest of about 1000 service strength tests with notched bars made of various materials, in which both form factor and mean stress were systematically varied and in which always the same load collective, namely the LBF standard distribution, was used (Ref.42).

To obtain a criterion for the extremely low damage sums, the stress amplitudes located below the fatigue limit were included into the Miner rule; for this, the Wöhler curve without discontinuity, with an exponent of k=6.8, was extended to the stress amplitude $\sigma_a=0$. A damage calculation, made with this

Wöhler curve, resulted in damage sums $\sum \frac{n_i}{N_i}$ of 0.5 - 2.2 at single-stage $\angle 20$

initial loading, while the corresponding values for a three-stage initial loading were 0.34 to 1.30 (see Table 8). The four- and five-stage service strength tests quite accurately yielded 1.0 (series 13a - c).

This means that the scattering width of the damage sums decreased considerably; in addition, about half of the values were above 1.0.

Conversely, the eight-stage service strength test furnished a value of only $\sum \frac{n_i}{N_i}$ = 0.37.

Thus, the fact that the normal Miner rule, in single-stage initial loading tests, resulted in such low damage sums can be attributed to its disregarding the stress amplitudes located below the fatigue limit (see the two columns in Table 8). The conditions are somewhat different for multistage initial loading tests and for service strength tests (see Table 8).

6. Experimental Procedure

Materials, test bars, testing machines, and statistical methods used have been described in detail in our earlier paper (Ref.1).

Translated for the National Aeronautics and Space Administration by the O.W.Leibiger Research Laboratories, Inc.